Optical Engineering

SPIEDigitalLibrary.org/oe

Effect of subsurface impurities of fused silica on laser-induced damage probability

Xiang Gao
Guoying Feng
Lingling Zhai
Zhou Shouhuan

SPIE

Effect of subsurface impurities of fused silica on laser-induced damage probability

Xiang Gao,[a] Guoying Feng,[a,*] Lingling Zhai,[a] and Zhou Shouhuan[a,b]
[a]Sichuan University, College of Electronic Information, Chengdu, Sichuan 610064, China
[b]North China Research Institute of Electro-Optics, Beijing 100015, China

Abstract. A thermal model coupled to statistics is proposed based on damage initiation by heating of size-distributed inclusions to a critical temperature. The data points of damage probability on the surface of fused silica containing different levels of impurities are measured. By linking the contents of various impurities measured to the calculation for damage probability, the influence of various impurities on damage probability is obtained. The purpose of the work is to present a more thorough analysis of the correlation of subsurface impurities to laser damage probability. [DOI: 10.1117/1.OE.53.2.026101]

Keywords: laser damage probability; polishing impurities; fused silica.

Paper 131486 received Sep. 30, 2013; revised manuscript received Dec. 11, 2013; accepted for publication Jan. 6, 2014; published online Feb. 4, 2014.

1 Introduction

For large-aperture, high-power laser systems, such as the National Ignition Facility in the United States,[1,2] Laser Megajoule in France,[3] and the SGIII laser facility in China,[4] the ultraviolet optical lifetime of fused silica must be increased. The polishing contaminants in the near-surface region of optical components can absorb sub-band gap light and produce a local heating that can initiate a material damage.[5] Many experimental facts have shown that absorbing nanometer-sized inclusions are responsible for the initiation of the damage process: an increase of the damage thresholds with purification of subsurface of fused silica;[6,7] a spatial variation of the damage threshold on the surface or in bulk of optical substrates;[8,9] and a dependence of the damage threshold on the irradiation spot-size and wavelength.[10,11] However, in most cases, the impurities are not identified by modern optical techniques since they are nanoscale size and are distributed at low concentration.[12]

It is obvious that the inclusion-initiated damage has a statistical character because of the spatial distribution of inclusions in a sample.[10] The theoretical studies of inclusion-initiated damage were based on the resolution of Fourier equation. [13–16] However, these models have not been substantiated enough to explain the statistical character in experiments. The information on damage density and damage threshold of precursors can be extracted from the experimental curves of damage probability.[11,17] Feit and Rubenchik have presented a model[18] that the size distribution of nanoabsorbers is related to the damage density and damage probability, which predicts the dependence of damage density on pulse duration.

In this paper, we go further to relate the contents of various impurities measured from the subsurface layers of different samples to damage probability. In Sec. 2, based on calculation of absorption of spherical particles and then solving the heat equation, for various particles, the critical fluence required to initiate damage can be calculated. Considering the fit distribution parameters, the laser damage probability on the surface of fused silica has been calculated. In Sec. 3, the subsurface components of impurities for different samples are determined by inductively coupled plasma optical emission spectrometry (ICP-OES) and the data points of laser damage probability have been measured. Subsequently, the theoretical model presented has been used for analyzing the effect of various impurities on damage probability.

2 Theoretical Model

2.1 *Critical Fluence*

Contaminants detected include the major polishing compound components (Ce or Zr from CeO_2 or ZrO_2), and other metals (Fe, Cu, Cr) induced by the polishing step or earlier grinding steps. Al is present largely because of the use of Al_2O_3 in the final cleaning process. Al_2O_3 and ZrO_2 are nonabsorbing materials at 355 nm, so we just consider CeO_2, Cu, Fe, and Cr particles in the simulation. With the improvement of surface-micromachining process, few 100-nm particles can be identified by classical optical techniques and can be removed from the subsurface of fused silica, so the particle radius of <100 nm was simulated in the model. For simplification, we only consider the shape of a sphere, although it is not necessarily needed in all cases.[19] The temperature distribution is necessary for evaluating the critical fluence required to initiate damage, and the spherical particle heating under the laser radiation is described by the equation of heat conduction.

$$C_i(T)\rho_i\frac{\partial T_i}{\partial t} = \nabla[\chi_i(T)\nabla T_i] + \frac{\sigma I}{V}f(t)\theta(R-r), \tag{1}$$

where ρ, $\chi(T)$, and $C(T)$ present density, thermal conductivity, and thermal capacity, respectively [values for T up to 2200 K (Ref. 19)]. I and $f(t)$ are maximum intensity

*Address all correspondence to: Guoying Feng, E-mail: guoing_feng@scu.edu.cn and temporal shape of laser pulse. A subscript i has two values: $i = p$ for an inclusion and $i = h$ for a host material. We consider a Gaussian temporal profile, $f(t) = \exp[-4(t^2/\tau^2)]$, for consistency with the experimental condition. $\theta(x)$ is a function defined as $\theta(x) = 0$ at $x < 0$ and $\theta(x) = 1$ at $x \geq 0$. σ is the absorption cross-section of the inclusion, and $V = (4/3)\pi R^3$ is the inclusion volume. The material thermal and optical parameters for calculation are exposed in Refs. 20 and 21. The absorption cross-section σ is calculated with the Mie theory.[22]

$$Q_{\mathrm{ext}} = \frac{2\pi}{k^2} \sum_{n=1}^{\infty} (2n+1) \mathrm{Re}(a_n + b_n), \tag{2}$$

$$Q_{\mathrm{sca}} = \frac{2\pi}{k^2} \sum_{n=1}^{\infty} (2n+1)(|a_n|^2 + |b_n|^2), \tag{3}$$

$$\sigma = Q_{\mathrm{ext}} - Q_{\mathrm{sca}}, \tag{4}$$

where Q_{ext} and Q_{sca}, respectively, are the extinction cross-section and scattering cross-section. $k = 2\pi N/\lambda$, where N is the optical index of host material and λ is the wavelength of irradiation. a_n and b_n are the scattering coefficients determined with continuity relations.

We plotted in Fig. 1 the absorption cross-section of various particles (CeO_2, Cu, Fe, and Cr) embedded in fused silica. We can see from Fig. 2 that the absorptivity of CeO_2 particles is much lower than others (Cu, Fe, and Cr) with the same size.

Considering the Fourier transform of the temperature, Eq. (1) can be written as

$$\frac{1}{r^2}\frac{\partial}{\partial r}\left(r^2 \frac{\partial \hat{T}_i}{\partial t}\right) + \alpha_i^2 \hat{T}_i = -\frac{\sigma I \theta(R-r)}{2V\chi_p(T)} \sqrt{\pi}\tau \exp\left(-\frac{\tau^2\omega^2}{16}\right), \tag{5}$$

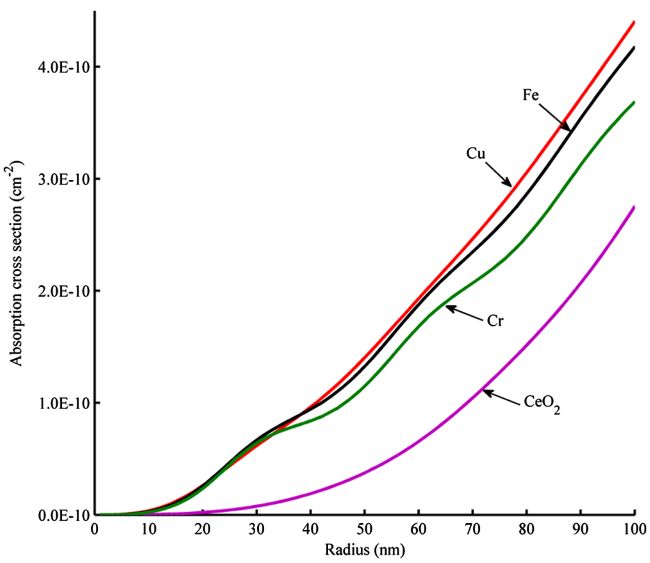

Fig. 1 The absorption cross-section calculated at 355 nm as a function of particle radius for various particles.

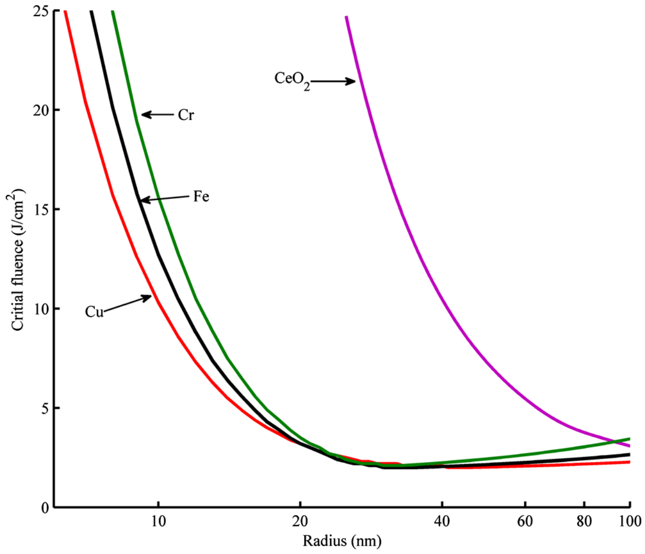

Fig. 2 Critical fluence calculated as a function of particle radius for various particles.

where $\alpha_i = [\omega\rho_i C_i(T)/2\chi_i(T)]^{1/2}(1+i)$. Applying the limit condition, the solutions can be expressed as

$$\hat{T}_p(r,\omega) = \frac{A_p I}{r}\left[\exp(i\alpha_p r) - \exp(-i\alpha_p r)\right] - \frac{\sigma I}{2V\alpha_p^2 \chi_p(T)} \sqrt{\pi}\tau \exp\left(-\frac{\tau^2\omega^2}{16}\right), \tag{6}$$

$$\hat{T}_h(r,\omega) = \frac{A_h I}{r} \exp(i\alpha_h r), \tag{7}$$

where A_p and A_h can be obtained by use of the boundary condition $[\hat{T}_p(R) = \hat{T}_h(R), \chi_p(T)\partial\hat{T}_p/\partial r|_{r=R} = \chi_h(T)\partial\hat{T}_h/\partial r|_{r=R})$. Then, the temperature T_i in the inclusion and host material can be obtained by numerical inverse Fourier transform. Damage is assumed to take place when maximum temperature at the particle–host material interfaces reaches a critical value (~2200 K).[23] Thus, the critical fluence F_c required to reach the critical temperature can be expressed as

$$F_c = \int_{-\infty}^{+\infty} I f(t) \mathrm{d}t = (\pi)^{\frac{3}{2}} R\tau T_c \left[\max_t\left(\sum_{\omega=-N}^{N} A_h \exp(i\alpha_h R - i\omega t)\Delta\omega\right)\right]^{-1}. \tag{8}$$

We consider that various particles embedded in fused silica are irradiated at 355 nm during pulse duration of 10 ns, and the critical fluence as a function of particle radius has been plotted in Fig. 2.

We can see from Fig. 2 that CeO_2 particles require higher fluence to initiate damage when the particle radius is <100 nm.

2.2 *Laser Damage Probability on the Surface of Optical Materials*

We assume that the breakdown is reached if a particle is irradiated with fluence higher than F_c, and the damage probability can be theoretically calculated based on the distribution law of particles. When the damage precursors are assumed to be subsurface inclusions, the laser damage probability can be expressed as a function of fluence F.[10]

$$P(F) = 1 - \exp\left[-\int_0^F g(F_c)S_{F_c}(F)\mathrm{d}F_c\right], \tag{9}$$

where $S_{Fc}(F)$ is the region within the spot size with fluence F greater than critical fluence F_c, $S_{Fc}(F) = (\pi\omega_0^2/2)\ln(F/F_c)$, with ω_0 the beam radius. $g(F_c)$ presents the number of defects per unit area that damage at fluence between F_c and $F_c + dF_c$. However, F_c depends on the particle size, and the size distribution of particles is unknown. Hence, we consider a power law distribution since this type of variation is typically found for clusters.[19]

$$n(R) = \frac{(\gamma - 1)d_0}{R_{\min}^{1-\gamma} - R_{\max}^{1-\gamma}} R^{-\gamma}, \tag{10}$$

where γ is a constant (its value often is 2 to 4 for natural processes, such as optics contamination[24]), and d_0 is the density of particles per unit of surface. Based on the relationship between critical fluence and particle size, the upper limit $R_{\max}$ can be obtained from measured damage threshold and the lower limit $R_{\min}$ can be obtained where the experimental damage probability is 1. The relationship between $g(F_c)$ and density of particles d_0 is

$$\int_0^\infty g(F_c)\mathrm{d}F_c = d_0. \tag{11}$$

With this model we have the ability to describe laser damage on the surface of fused silica as function of fluence F by choosing two physical characteristics: the size distribution of particles γ and their density d_0 on the subsurface of optical materials. By choosing the fit distribution parameters d_0 and γ, we can insert the $R_{\min}$ and $R_{\max}$ from sample S1 (see Table 1) to calculate the laser-induced damage probability based on the relationship between critical fluence and particle radius.

Figure 3 shows that damage probability initiated by CeO_2 particles increases as the density of particles d_0 increases, and decreases as the parameter of size distribution γ increases. In order to identify the influence of various particles on damage probability, we plotted in Fig. 4 the curves of laser damage probability initiated by various particles calculated with same parameters $d_0 = 1 \times 10^6$ mm^2 and $\gamma = 3$. From Fig. 4, we can see that considering the size distribution from sample S1 as seen in Table 1, CeO_2 particles have a greater damage probability than others (Cu, Fe, and Cr) with the same distribution parameters d_0 and γ.

Table 1 The values for $R_{\min}$ and $R_{\max}$ of different particles from samples S1 to S4.

$R_{\min}$, $R_{\max}$ (nm)	CeO_2	Cu	Fe	Cr
S1	37, 50	9, 13	11, 15	13, 16
S2	33, 45	8, 11	10, 13	12, 14
S3	32, 38	7, 10	9, 12	11, 13
S4	30, 36	6, 9	8, 11	10, 12

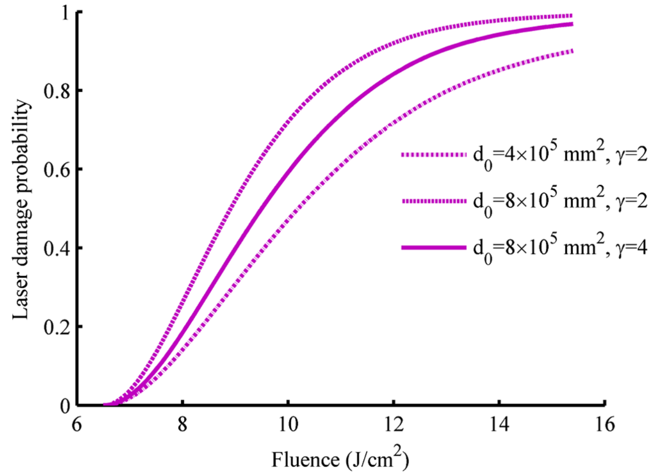

Fig. 3 Laser damage probability initiated by CeO_2 particles with different distribution parameters d_0 and γ.

3 Experiment

The experimental setup for laser-damage test has been described in detail elsewhere,[11,17] and only a brief description is given here. The data points of laser damage probability are measured at 355 nm using injected Nd:YAG laser with the Gaussian temporal profile. The effective pulse duration (at $1/e$) is 10 ns. In order to obtain typical damage probability in larger range of fluence, the small spot diameter of 8 μm (at $1/e^2$) is chosen in the test. The error of

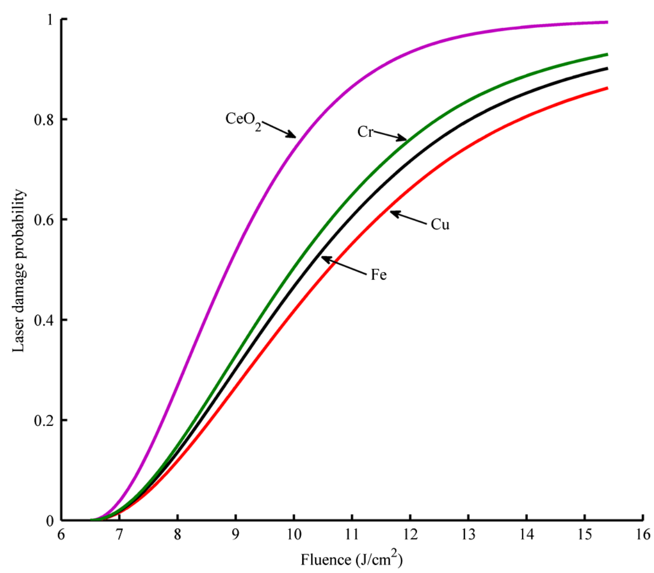

Fig. 4 Laser damage probability initiated by various particles with same distribution parameters ($d_0 = 1 \times 10^6$ mm^2 and $\gamma = 3$).

measured spot diameter is ∼140 nm. The damage test 1-on-1 is applied with a large number of points to obtain a reliable measurement. We observe the 50 different regions under the laser irradiation at each fluence F, and each data point $P(F)$ is plotted by counting the number of damage regions at each fluence F. Energy of the incident beam is measured with a calorimeter, and the fluence fluctuations have a standard deviation of ∼10%. To have a good accuracy of measurement, the test procedure of damage probability is repeated 10 times and the deviation $\triangle P$ of average value is <0.08. In order to identify the effect of the contents of various impurities on laser damage probability, the components of impurities from subsurface layer are determined by ICP-OES and the data points of damage probability have been measured.

The fused silica samples (S1, S2, S3, S4) polished by cerium oxide slurry with different polishing levels were used in the experiment. Because of insufficient polishing process, there are more structural defects (per area), such as submicroscopic cracks, pores, and indentations, observed on the surface of samples S3 and S4. The size of the samples is $35 \times 35 \times 3$ mm. After accurate weighing and thickness measurement, ∼1 μm of fused silica was digested by ultrapure grade hydrofluoric acid solution during 7 min. The masses of subsurface layer digested, respectively, were 0.00215, 0.00243, 0.00256, and 0.002695 g. The contents of impurities can be obtained by suitable spectral analysis. The contents of CeO_2 and Al_2O_3 incorporated during polishing and cleaning process can be calculated based on the contents of Ce and Al measured by ICP-OES. Table 2 gives the contents of main impurities from the subsurface layer.

We can see from Table 2 that the contents of CeO_2 impurities have much more than others and have large distinction in different samples. In order to relate the contents of various impurities to damage probability, the impurities are assumed to be spherical and their mass m (per area) has a homogeneous distribution on the subsurface of fused silica. Thereby, the density (per area) of particles d_0 can be calculated from Eq. (10).

$$d_0 = \frac{m}{\rho S}\left[\int_{R_{\min}}^{R_{\max}} \frac{4}{3}\pi \frac{(\gamma-1)}{R_{\min}^{1-\gamma} - R_{\max}^{1-\gamma}} R^{3-\gamma} \mathrm{d}R\right]^{-1}, \tag{12}$$

where S is the surface area of the samples and ρ is the mass density of the particles. In order to make the shape of damage probability curves more consistent with experimental data, the parameter γ is set to 3. The values for $R_{\min}$ and $R_{\max}$ of different particles, which are used in the calculation, can be obtained based on the description in Sec. 2.1, and they have been summarized in Table 1 from samples S1 to S4. Then, according to the critical fluence as a function of particle radius as seen in Fig. 2, the damage density $g(F)$ can be expressed as[25]

$$g(F) = \int_{R_{\min}}^{R_{\max}} n(R)\mathrm{d}R. \tag{13}$$

Substituting Eq. (13) into Eq. (9), the curves of damage probability from samples S1 to S4 can be calculated. The scheme for calculation has been presented in Fig. 5.

Figure 6 shows the experimental data points of damage probability measured on the surface of fused silica and theoretical curves initiated by impurities. As seen in Fig. 6, the smaller particle is required to absorb more fluence to reach breakdown. Thus, the damage threshold increases from samples S1 to S4 because the upper limit $R_{\max}$ decreases as seen in Table 1. Cu and Cr impurities have a very weak influence on experimental damage probability since their contents on the subsurface of the samples are very low. On the contrary, CeO_2 and Fe impurities are closely related to the damage probability when the levels of contents are high as seen in sample S1. We can also notice that for the samples with low CeO_2 contents (S2, S3, and S4), this correlation is weaker, and it has a good agreement with experimental data on CeO_2 contents dependence of damage density.[26] In the case of CeO_2 impurities, as the dramatic decrease of the contents from samples S1 to S4, the damage density will decrease according to our calculation. As a consequence, the damage probability induced by the laser pulse with same fluence will decrease. Obviously, a large discrepancy is found between theory and experiment in samples S3 and S4 since there are more structural defects located on the subsurface of samples from insufficient polishing process. These structural defects with a spatial distribution add the absorbing centers near the surface[27] and cause more damage sites than expected from the distribution of impurities, so the

Table 2 The contents of main impurities from subsurface layer of fused silica (μg/g).

Sample	CeO_2	Cu	Fe	Al_2O_3	Cr
S1	1484.2	17.6	37.1	19.4	16.4
S2	937.3	15.2	27.3	17.3	8.6
S3	638.9	12.8	39.2	22.6	13.2
S4	333.8	6.68	23.5	15.4	5.6

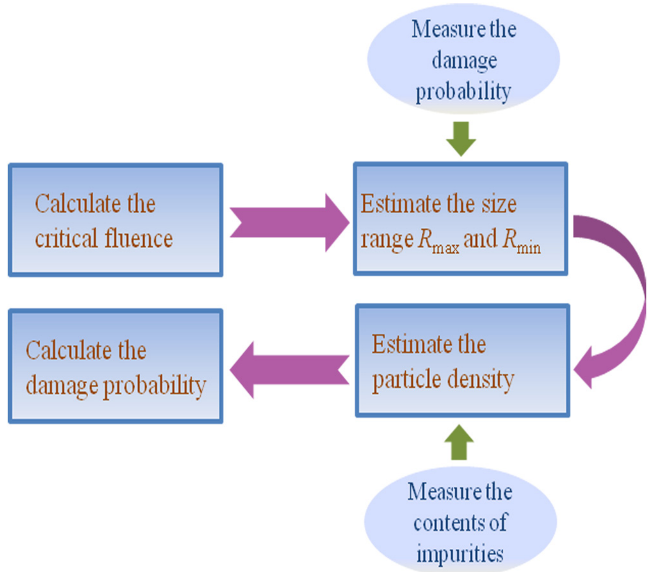

Fig. 5 The scheme for calculating damage probability.

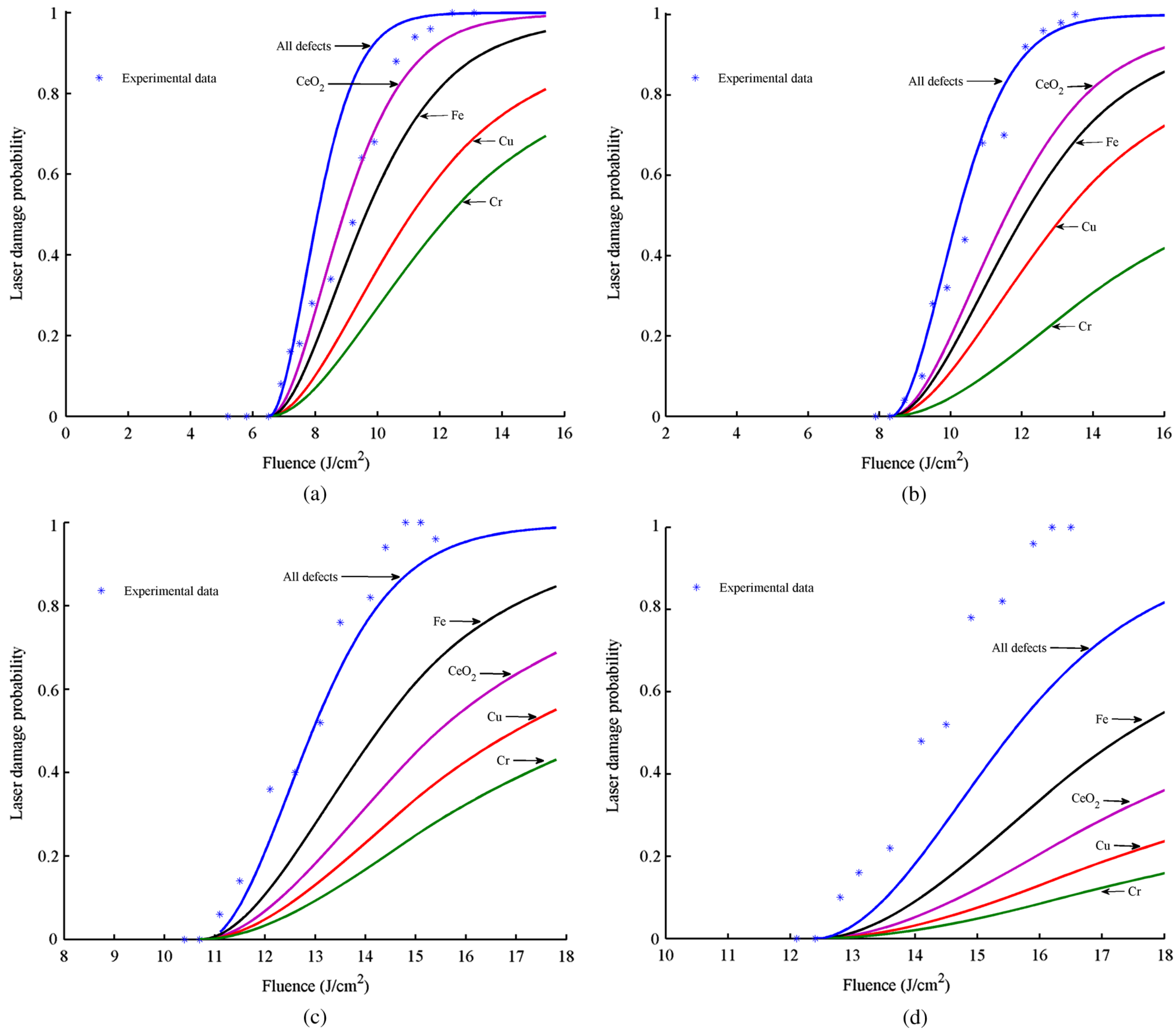

Fig. 6 The data points of damage probability measured on the surface of fused silica and theoretical curves initiated by impurities for different samples. (a) S1. (b) S2. (c) S3. (d) S4.

measured laser damage probability is found to be larger than theoretical calculation.

4 Conclusion

A model has been presented in order to relate the distribution properties of various impurities on the subsurface of fused silica to damage probability. The theoretical curves of damage probability initiated by the impurities having a given density and size distribution have been obtained. The data points of damage probability on the surface of fused silica have been measured. Meanwhile, the contents of impurities from the subsurface layer of fused silica have been determined by ICP-OES. The correlation of different contents of impurities to damage probability has been analyzed, and it has a good agreement with obtained results. This model is of interest for identifying the influence of various impurities induced by polishing, grinding, and cleaning processes on laser damage probability, and it can also be applied to investigate laser damage on surface of other optical substrates or films.

Acknowledgments

This work was supported by Major Program of National Natural Science Foundation of China (60890200) and National Natural Science Foundation of China (10976017).

References

1. A. Conder et al., "Final optics damage inspection (FODI) for the National Ignition Facility," *Proc. SPIE* **6720**, 672010 (2007).
2. C. A. Haynam et al., "National Ignition Facility laser performance status," *Appl. Opt.* **46**(16), 3276–3303 (2007).
3. N. Fleurot, C. Cavailler, and J. L. Bourgade, "The Laser Mégajoule (LMJ) Project dedicated to inertial confinement fusion: development and construction status," *Fusion Eng. Des.* **74**(1–4), 147–154 (2005).
4. H. S. Peng et al., "Design of 60-kJ SG-III laser facility and related technology development," *Proc. SPIE* **4424**, 98–103 (2001).
5. B. Bertussi, J. Y. Natoli, and M. Commandre, "Effect of polishing process on silica surface laser-induced damage threshold at 355 nm," *Opt. Commun.* **242**(1–3), 227–231 (2004).
6. I. S. Tayyab et al., "HF-based etching processes for improving laser damage resistance of fused silica optical surfaces," *J. Am. Ceram. Soc.* **94**(2), 416–428 (2011).
7. J. A. Menapace et al., "Combined advanced finishing and UV-laser conditioning for producing UV-damage-resistant fused-silica optics," *Proc. SPIE* **4679**, 56–68 (2002).

8. J. Y. Natoli et al., "Laser-induced damage of materials in bulk, thin-film, and liquid forms," *Appl. Opt.* **41**(16), 3156–3166 (2002).
9. H. Krol, "Investigation of nanoprecursors threshold distribution in laser-damage testing," *Opt. Commun.* **256**(1–3), 184–189 (2005).
10. L. Gallais et al., "Investigation of nanodefect properties in optical coatings by coupling measured and simulated laser damage statistics," *J. Appl. Phys.* **104**(5), 53120–53129 (2008).
11. X. Gao et al., "Investigation of laser-induced damage by nanoabsorbers at the surface of fused silica," *Appl. Opt.* **51**(13), 2463–2468 (2012).
12. M. R. Kozlowski et al., "Depth profiling of polishing-induced contamination on fused silica surfaces," *Proc. SPIE* **3244**, 365–375 (1997).
13. L. Gallais, P. Voarino, and C. Amra, "Optical measurement of size and complex index of laser-damage precursors: the inverse problem," *J. Opt. Soc. Am. B.* **21**(5), 1073–1080 (2004).
14. R. Hopper and D. Uhlmann, "Mechanism of inclusion damage in laser glass," *J. Appl. Phys.* **41**(10), 4023–4037 (1970).
15. A. Dyan et al., "Scaling laws in laser-induced potassium dihydrogen phosphate crystal damage by nanosecond pulses at 3ω," *J. Opt. Soc. Am. B.* **25**(6), 1087–1095 (2008).
16. M. F. Koldunov and A. A. Manenkov, "Theory of laser-induced inclusion-initiated damage in optical materials," *Opt. Eng.* **51**(12), 121811 (2012).
17. L. Gallais, J. Y. Natoli, and C. Amra, "Statistical study of single and multiple pulse laser-induced damage in glasses," *Opt. Express* **10**(25), 1465–1474 (2002).
18. M. D. Feit and A. M. Rubenchik, "Implications of nanoabsorber initiators for damage probability curves, pulselength scaling, and laser conditioning," *Proc. SPIE* **5273**, 74–82 (2003).
19. J. B. Trenholme, M. D. Feit, and A. M. Rubenchik, "Size-selection initiation model extended to include shape and random factors," *Proc. SPIE* **5991**, 9910–9922 (2005).
20. T. Y. Steven et al., "Thermal transport in CO_2 laser irradiated fused silica: In situ measurements and analysis," *J. Appl. Phys.* **106**(10), 103106 (2009).
21. M. J. Weber, *Handbook of Optical Materials*, CRC, Florida (2002).
22. H. C. Hulst, *Light Scattering by Small Particles*, Wiley, New York (1957).
23. J. Bude et al., "The effect of lattice temperature on surface damage in fused silica optics," *Proc. SPIE* **6720**, 672009 (2007).
24. U. Kreibig and M. Vollmer, *Optical Properties of Metal Clusters*, Springer, New York (1995).
25. X. Fu et al., "Investigation of the distribution of laser damage precursors at 1064 nm, 12 ns on niobia-silica and zirconia-silica mixtures," *Opt. Express* **20**(23), 26089–26098 (2012).
26. J. Neauport et al., "Polishing induced contamination of fused silica optics and laser induced damage density at 351 nm," *Opt. Express* **13**(25), 10163–10171 (2005).
27. M. D. Feit, "Influence of subsurface cracks on laser-induced surface damage," *Proc. SPIE* **5273**, 264–272 (2004).

Xiang Gao received his BS degree from the Department of Applied Physics at Sichuan University of Science & Engineering in July 2009. Then, he was admitted to Sichuan University to pursue a PhD in optical engineering in 2011. His research work mainly focus on nanosecond/femtosecond laser–matter interactions at high intensities. Now he has published 11 papers in journals.

Guoying Feng graduated from Zhejiang University, Department of Optical Engineering, in 1969. She received a PhD degree in laser technology from Zhejiang University of College of Electronic Information in 1998. Her research is focused on laser physics and technology, laser beam propagation and control, laser-induced damage, etc. She published over 100 scientific papers in journals, conference proceedings, and books. She is also a professor in the Department of Optical Engineering of Sichuan University.

Lingling Zhai received her bachelor's degree in 2007. She is currently enrolled in the College of Electronics and Information Engineering at Sichuan University and will receive a master's degree in engineering in 2014. Her research area is laser-induced damage in optical components, particularly, fused silica. In 2013, she published a paper about laser damage mechanism induced by inclusions in fused silica in high-power laser and particle beams.

Zhou Shouhuan suggested the technical implementation idea of DPSSL and became one of the earliest researchers of DPSSL in China in the beginning of 1970s. He has won the Second Grade National Invention Prize and the Second Grade of the National Prize for Progress in Science and Technology. He was elected member of the Chinese Academy of Engineering in 2003.